

Analog active valve control design for non-linear semi-active resetable devices

Geoffrey W. Rodgers, J. Geoffrey Chase* and Sylvain Corman

Department of Mechanical Engineering, University of Canterbury, Private Bag 4800, Christchurch, New Zealand

(Received August 11, 2016, Revised February 3, 2017, Accepted February 13, 2017)

Abstract. Semi-active devices use the building's own motion to produce resistive forces and are thus strictly dissipative and require little power. Devices that independently control the binary open/closed valve state can enable novel device hysteresis loops that were not previously possible. However, some device hysteresis loops cannot be obtained without active analog valve control allowing slower, controlled release of stored energy, and it presents an ongoing limitation in obtaining the full range of possibilities offered by these devices. This *in silico* study develops a proportional-derivative feedback control law using a validated nonlinear device model to track an ideal diamond-shaped force-displacement response profile using active analog valve control. It is validated by comparison to the ideal shape for both sinusoidal and random seismic input motions. Structural application specific spectral analysis compares the performance for the non-linear, actively controlled case to those obtained with an ideal, linear model to validate that the potential performance will be retained when considering realistic nonlinear behaviour and the designed valve control approach. Results show tracking of the device force-displacement loop to within 3-5% of the desired ideal curve. Valve delay, rather than control law design, is the primary limiting factor, and analysis indicates a ratio of valve delay to structural period must be 1/10 or smaller to ensure adequate tracking, relating valve performance to structural period and overall device performance under control. Overall, the results show that active analog feedback control of energy release in these devices can significantly increase the range of resetable, valve-controlled semi-active device performance and hysteresis loops, in turn increasing their performance envelope and application space.

Keywords: nonlinear; control; design; semi-active; earthquake; energy dissipation; valve control

1. Introduction

Semi-active control is an effective potential method of mitigating structural damage from large environmental loads. Significant response reductions (Bobrow *et al.* 2000, Jabbari and Bobrow 2002, Caterino *et al.* 2015, Dyke and Spencer 1996, Esteki *et al.* 2015, Ewing *et al.* 2009, Woo *et al.* 2011, Yang and Agrawal 2002, Yang *et al.* 2007, Zhang and Agrawal, 2015, Jansen and Dyke, 2000, Bitaraf *et al.* 2010a, Bitaraf *et al.* 2012, Bitaraf and Hurlebaus 2013, Ozbulut *et al.* 2011) can be obtained with low-power requirements, a strictly dissipative input guaranteeing stability, and a broad range of control and robustness to structural parameter changes. These are outcomes that tuned, passive systems cannot typically provide (Barroso *et al.* 2003, Chase *et al.* 2004, Chase *et al.* 2006, Rodgers *et al.* 2007, Jansen and Dyke 2000, Kim *et al.* 2010).

One of the most common semi-active devices considered is the magneto-rheological (MR) damper (Dyke and Spencer 1996, Spencer *et al.* 1997). This device can create high resistive and dissipative forces, and a range of behaviours obtained, either alone or in combination with passive devices (e.g., (Bitaraf *et al.* 2010b, Esteki *et al.* 2015, Maiti *et al.* 2006, Spencer *et al.* 2000, Bitaraf *et al.*

2010a, Bitaraf *et al.* 2012, Bitaraf and Hurlebaus 2013)). However, they are relatively high cost systems, and their performance has not yet been able to be customised within each quadrant of a hysteresis, force-displacement loop.

Equally, a range of variably controlled tuned mass dampers and isolation systems, have offered the ability to partially customise the hysteresis loop of the overall structure via variable stiffness, friction and damping devices (Feng 1993, Feng *et al.* 1993, Kori and Jangid 2008, Nagarajaiah and Jung 2014, Sun *et al.* 2014, Ozbulut and Hurlebaus 2012b). Equally, a range of smart materials and variable friction devices with a range of device control have also been proposed (e.g., (Ozbulut and Hurlebaus 2010, Ozbulut and Hurlebaus 2011b, Ozbulut and Hurlebaus, 2011a, Ozbulut and Hurlebaus 2012a)). In both cases, the ability to directly customise device and/or structural hysteresis in each quadrant is not yet readily achieved.

Another specific class, semi-active resetable devices are hydraulic or pneumatic spring elements with a resetable unstretched spring length that dissipate stored energy through binary on/off controlled valves (Bobrow *et al.* 2000, Chase *et al.* 2006, Chen *et al.* 2008, Jabbari and Bobrow 2002, Yang *et al.* 2007), adding nonlinear stiffness without altering the inherent structural damping. In these devices, a piston displacement stores energy by compressing a working fluid. Release of all the stored energy via actively controlled valves being opened (on/off or binary control) at peak displacement or peak velocity, semi-actively dissipates stored structural response energy. However, and

*Corresponding author, Distinguished Professor
E-mail: geoff.chase@canterbury.ac.nz

importantly, if each chamber of a resetable device, on either side of the device piston, is independently controlled with its own set of valves it offers the unique opportunity to sculpt or re-shape the structural hysteresis loop to specific shapes to better meet design needs (Chase *et al.* 2006, Mulligan *et al.* 2010, Chen *et al.* 2008).

Importantly, these specific shapes, as illustrated in Fig. 1(a)-1(c), are currently limited to what is possible with on/off binary valve behavior for storing and releasing energy. The 1-4 and 2-4 devices, in particular (Figs. 1(b) and (c)) are well-known with both analytical and experimental quantification of their potential benefits and limitations (Barroso *et al.* 2003, Bobrow *et al.* 2000, Chase *et al.* 2004, Chase *et al.* 2006, Mulligan 2007, Mulligan *et al.* 2009, Mulligan *et al.* 2010, Rodgers *et al.* 2007, Yang and Agrawal 2002, Yang *et al.* 2007, Chen *et al.* 2008).

They are also relatively simple devices, where 1-4 and 2-4 control laws require only displacement feedback data for motion across the device to determine position and velocity, defining the current quadrant of the displacement-velocity plot, and thus the required binary open/closed control of the valve state.

The 2-4 device advantages in reducing base shear are limited by reduced reductions in displacement (Rodgers *et al.* 2007). Active analog, rather than binary, valve control would provide greater dissipation and thus greater displacement response reduction, but is not yet possible with these devices or MR dampers (Spencer *et al.* 1997, Chen *et al.* 2015, Som *et al.* 2015, Zhou *et al.* 2012). This research adds analog valve control to increase displacement reductions, while maintaining base shear reductions, a limiting factor in adding devices to any structure (Chen *et al.* 2008, Beziat *et al.* 2012, Makris and Chang 2000, Ramallo *et al.* 2002).

Fig. 1(d) shows a device hysteresis loop that resists motion from a peak value towards zero like a 2-4 device, but uses analog valve control in quadrants 1 and 3, as the structure motion moves away from equilibrium, to control or limit the energy release compared to a simple on/off valve. This approach augments the 2-4 control law and yields diamond-shaped force displacement behaviour, denoted a “diamond” device. This approach significantly expands the utility of these devices, but only if the nonlinearity of the device fluid flow can be adequately modeled and controlled, particularly using a relatively simple control law that does not rely on excessive feedback sensor information, minimising complexity and maximising robustness.

Validated nonlinear models (Mulligan *et al.* 2010) and experiments (Mulligan *et al.* 2009) indicate the desired linear behaviour in quadrants 2 and 4 in Fig. 1(d) is difficult to achieve, and will thus also require active analog control of the valves in each chamber to obtain the ideal device response shown when using a real device. The desired behaviour in quadrants 1 and 3 also requires actively controlled valves to linearize resistive forces and obtain the ideal hysteresis loop shape, minimising inherent nonlinear device dynamics (Mulligan *et al.* 2010). In addition to displacement information across the device, this goal also requires pressure measurements in both chambers, allowing

the resistive device force for a given working fluid (air or fluid) to be calculated so the necessary release rate through the valves can be determined to obtain the desired force-displacement response behaviour. These pressure measurements are readily available with typical, relatively low cost sensors.

Finally, it is important to note that analog valve control can be implemented either directly with analog valves with controllable orifice opening diameter, or indirectly using a series of binary controlled on/off valves. In the simpler latter case, a cluster of independently controllable binary stable valves can provide the desired result relatively more simply. More specifically, the controller determines the required valve area, and obtains it by opening the relevant fraction of (smaller) binary valves. This option is only limited by space for the valves and the relative size of each determining the resolution that is possible. Thus, the overall approach examined in this work can be obtained either way, where the latter approach is potentially simpler and more robust to design and control.

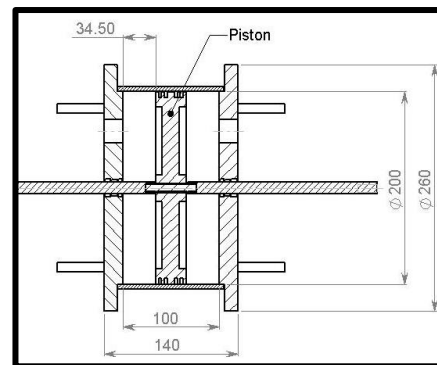
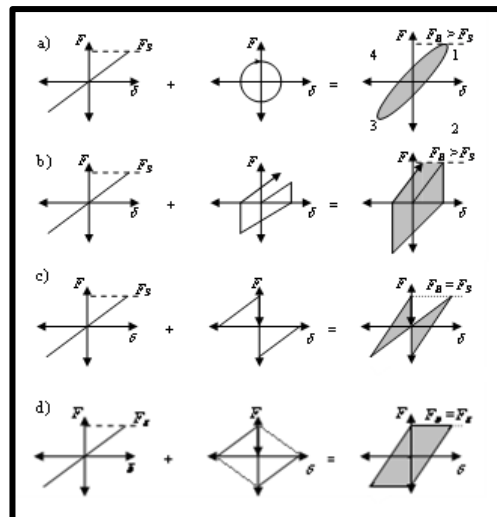


Fig. 1 Schematic force-displacement hysteresis loops for: (a) passive viscous damper for comparison, (b) a 1-4 device, (c) a 1-3 device, and (d) a 2-4 device. Note that F_B = total base shear of the structure, and F_S = base shear for a linear, undamped structure. Thus, $F_B > F_S$ indicates an increase in total base shear due to the additional device reaction loads. Semi-active device design schematic showing independent chamber control valve outlets

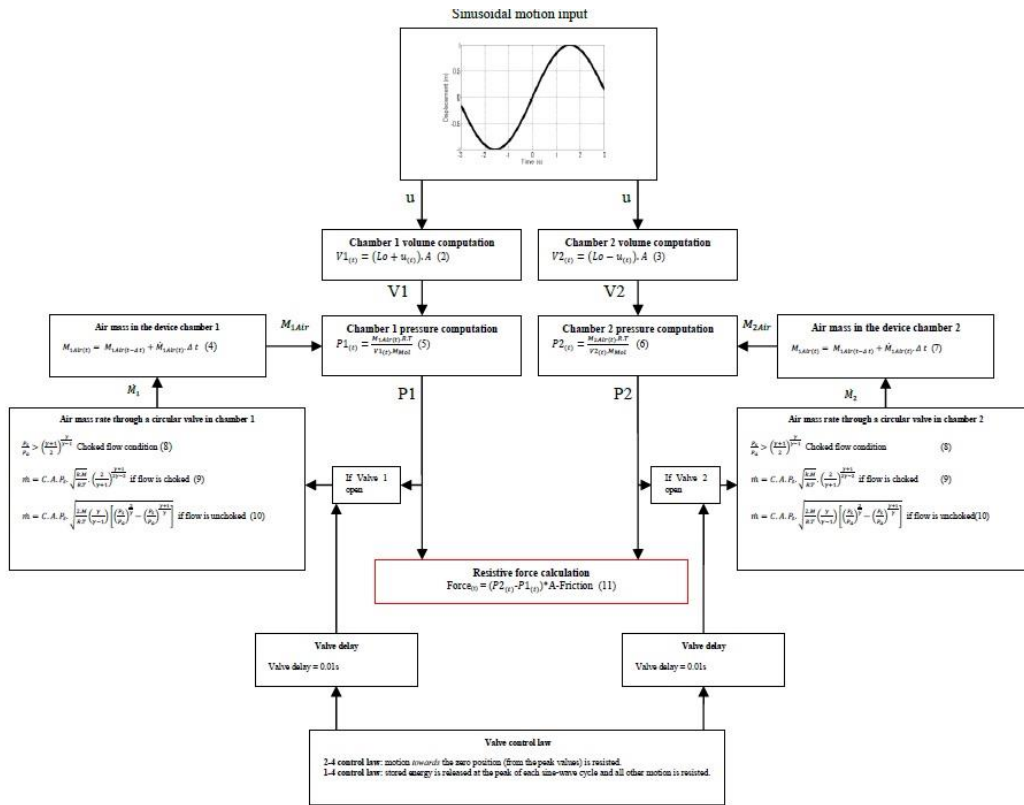


Fig. 2 Complete Nonlinear Model for Semi-Active Device shown within the schematic of its usage and mechanics for greater clarity of what equations govern which behaviour

Hence, the primary issue preventing greater use and capability of these devices revolves around the need for analog active valve control design, rather than a specific limitation in the device or sensors available. This research uses a validated nonlinear model as the foundation of a model-based design process to develop a control system to produce a diamond-shaped control law for resetable devices. To validate this feedback control approach and its potential in application, comparisons are made between linear and nonlinear models for:

- Sinusoidal input motion, to show best case performance and proof of concept
- Random earthquake inputs, to show realistic case performance

Finally, spectral analyses per the works of Rodgers *et al.* (Rodgers *et al.* 2007) are performed to demonstrate its potential aseismic performance to those of the 1-4 and 2-4 device cases, and justify the potential of adding this level of complexity to the device and structural application. This study considers devices with air as the working fluid, per prior studied and validated prototypes (Chase *et al.* 2006, Mulligan *et al.* 2009, Mulligan *et al.* 2010). However, more complex designs using hydraulic (or similar) working fluids are equally possible, as the validated models used here and the work presented are readily generalised to these cases.

The overall work is thus the design and analysis of an analog active valve controller system to enable a far wider application of these nonlinear, but effective, resetable seismic energy dissipation devices.

2. Device modelling and dynamics

2.1 Nonlinear device model

The nonlinear model used here was developed in (Mulligan 2007, Mulligan *et al.* 2009, Mulligan *et al.* 2010) and validated with data from experimental prototypes (Mulligan *et al.* 2009, Mulligan *et al.* 2010). For clarity and simplicity, Fig. 2 shows the model equations inside the computational flow for a sinusoidal input (Mulligan *et al.* 2010). Full derivations and validation are not in the scope of this study, and are presented in (Mulligan *et al.* 2010).

Summarising Fig. 2, the ambient temperature, T , is taken as 293°K and the air molar mass, M_{mob} , is 0.02897 Kg.mol⁻¹. From these constants, the input displacement enables calculation of each chamber volume using Eqs. (2) and (3). Eqs. (5) and (6) yield a resulting chamber pressure using the ideal gas law, with $R = 8.31 \text{ J.mol}^{-1} \cdot \text{K}^{-1}$ for a working fluid of air but generalisable to other fluids and values. These pressures enable calculation of the mass flow rate, using Eqs. (8)-(10), where the mass flow rate depends on the valve state. The valve state is defined by the valve control law and any valve delay in implementing a control signal. Thus, working backwards, a force-displacement trajectory can be tracked by controlling the mass flow rate using active valve control.

Valve delay is critical in these devices (Mulligan *et al.* 2010) and comprises the total delay between the command signal being sent to the valve and eventual completed valve

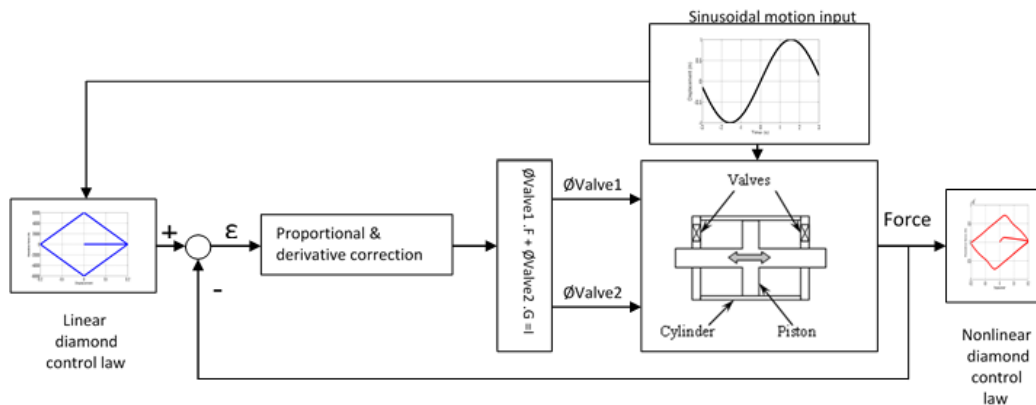


Fig. 3 Diamond shape control feedback control. Example shows a sinusoidal motion input

response, an electro-mechanical delay. It is not a constant, but a function of the valve used and the pressure inside the chamber with respect to the valve rating. In this study, an average value of 0.01s is used based on prior experimental work (Mulligan *et al.* 2010), but is varied to assess the sensitivity of performance to this sensitive and critical parameter.

The air mass rate is used in Eqs. (4) and (7) to calculate the increase/decrease in pressure between the inside chamber and the outside. The pressure difference between the chamber and the ambient or fluid reservoir pressure is then reused in the pressure computations in Eqs. (5) and (6). Finally, the resistive force is calculated from the pressure difference between the chambers (Bobrow *et al.* 2000, Chase *et al.* 2006) and the device friction force. The friction force was set at 500N (Mulligan *et al.* 2010) in this study using Eq. (11), but can be set to any realistic or device-specific value. This overall computational loop in Fig. 2 can readily be used to model any similar nonlinear device or resettable devices with other working fluids.

2.2 Active valve control

To obtain the active valve control, the valve diameter needs to be calculated only for the working chamber. The active chamber is the one currently expelling air or fluid from the device to atmosphere or an accumulator. Valve(s) on the non-working side are set to create the maximum opening and minimal resistance to permitting any air/fluid to leave to avoid unwanted increased pressures above atmospheric that reduce the total device force (Chase *et al.* 2006, Mulligan *et al.* 2010).

Fig. 3, shows the block diagram for controlled output resistive force tracking the projected linear trajectory, per Eq. (11) in Fig. 2. At each time step, the difference of the device force and desired linear, ideal trajectory are given to a proportional and derivative (PD) feedback controller. Working backwards in Fig. 2, Eqs. (8) to (10) then give the necessary air mass flow rate for each chamber, proportional to pressure and valve diameter. As the valve delay is fixed in a given simulation, the release rate capacity of each valve can be calculated as the air mass released during that valve

delay time period assuming a constant shaft speed over that same delay period. This assumption is likely acceptable for a small delay of 0.01s relative to typical structural periods of 1.0-3.0 seconds. Thus, an ideal valve diameter can be calculated at each time step as the command input to the valve(s) in the active chamber.

The PD control gains are found empirically using an iterative design method. The derivative control gain is set to zero and the proportional gain is slowly increased until reaching a stability limit. The derivative gain is then slowly increased until instability disappears. Integral control for correcting small errors was investigated, but added insignificant performance for the added complexity. Thus, the PD controller was selected as a simplest, robust solution approach to maximise the overall robustness of the final system.

This approach is acceptable for sinusoidal inputs. However, in a random seismic input case, there can be small response reversals without crossing zero displacement across the device. In particular, with a random input it is not possible to know when the motion will reverse, unlike in the sinusoidal case. It is thus not possible to know exactly how rapidly or slowly to release the stored energy in controlling the active device chamber for a random input, as opposed to a regular and predictable sinusoidal case. Note that for 1-3 and 2-4 devices this issue is not important as release rates are always maximised.

For simplicity, the control scheme presented keeps the slope for energy release in quadrants 1 and 3, the same, but with opposite sign, as that in quadrants 2 and 4. This choice is made for lack of better information, and thus assumes that the current response cycle will maintain a similar amplitude of motion as the prior response cycle. This assumption is not perfect, as seen in the drop-offs in the loop in some cycles for a simulated ideal linear diamond shaped device and a random earthquake input in Figure 4. However, it maintains simplicity in control design and requires only this previous slope be kept. Thus, a release rate and valve size can be calculated readily based on the prior part of the response cycle, as the future size of a half-cycle of response cannot be predicted for a random input.

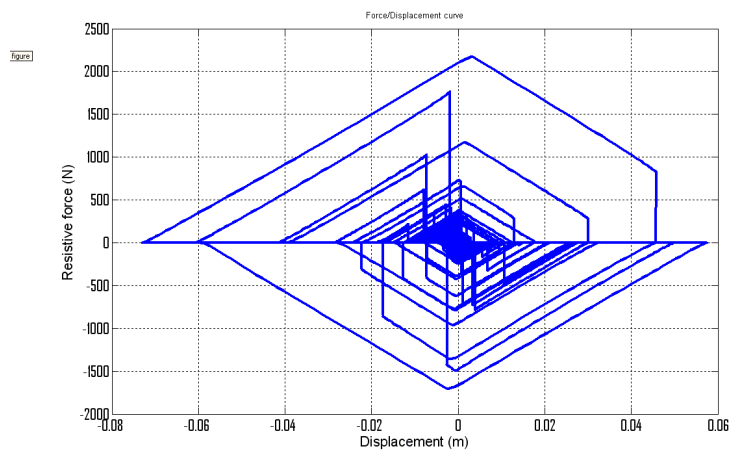


Fig. 4 Typical ideal, linear force/displacement diamond control law device hysteresis loop for a random seismic input case

At this point, there are two cases. First, the motion suddenly changes direction, but the resistive force is still nonzero. In this case, the opening of the valves is reversed, the remaining stored energy is immediately released from the active chamber, and (on valve closure) begins to increase in the opposite, now active chamber. In the second case, the force reaches zero, but the motion continues in the same direction. In this case, the valve(s) remain open at their maximum size and minimum resistive force and wait for a change in direction of the motion. These two cases cover the situation where the motion reverses with smaller amplitude than the prior cycle (first case), and where it has a larger subsequent amplitude (second case). Both cases are evident in Fig. 4. While simple, it is readily implemented and thus ideal for this proof of concept analysis.

2.3 Structure-device model

This feedback control of valve area seeks to obtain the linear ideal behaviour from the nonlinear, real device. To assess potential impact on structural response in comparison to the ideal case, and thus determine whether the control approach is effective if used with real, inherently nonlinear devices, a simple, linear structure with device can be modelled as a single degree of freedom mass with an internal viscous damping of 5%. Such models capture most building response, as most buildings are first (vibration) mode dominant in seismic response (90-99%) in each direction. This simple model and approach is effective at capturing the expected response, or changes when devices are added, and is thus commonly used by design codes and standards as part of spectral analyses used in initial building design (Chopra 1995).

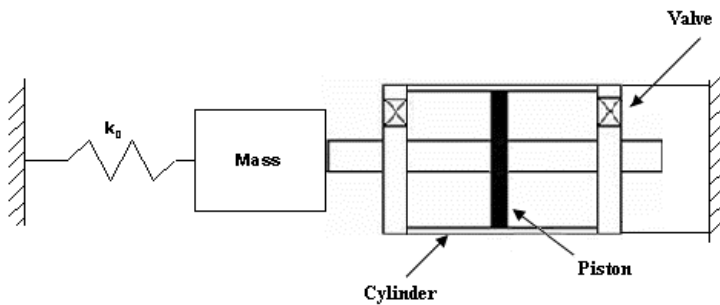
3. Analysis and Validation

The following analyses are used for validation of the control law and its efficacy:

1. **Analysis 1:** Sinusoidal input motions are imposed on the nonlinear model to assess best achievable performance in terms of input frequency (device velocity) and amplitude. Results are compared to the ideal, linear model case to assess how well the control system provides the desired, ideal output. The device design and size parameters are shown in Fig. 1 and are the same as those used in (Mulligan *et al.* 2009, Mulligan *et al.* 2010).
2. **Analysis 2:** Spectral analysis for 60 earthquakes from the SAC ground motion suite (Sommerville *et al.* 1997) using the nonlinear device model in a standard single degree of freedom linear structure, shown schematically in Table 1 with the structural parameters, to assess the potential to reduce structural response to random, seismic inputs that provide random, time varying device velocity and motion inputs. The ground motions were not pre-processed in any way, and were used directly for this analysis. The resettable device stiffness is set to 100% column stiffness for easy comparison to prior work (Rodgers *et al.* 2007), and both the nonlinear model and ideal linear diamond shaped control law models are used, where comparison assesses the impact of imperfectly controlled nonlinear device behaviour. The device models in both cases are scaled to achieve the 100% of column stiffness value for the device when controlled to a linear behaviour. The average structural force and base shear force over all 60 events are assessed as reductions factors from the uncontrolled baseline case per (Rodgers *et al.*, 2007), and thus compared to the performance of 1-4 and 2-4 devices in the same analysis from (Rodgers *et al.* 2007).

Response spectra (**Analysis 2**) are a standard performance based design tool for structural design, and illustrate how performance would vary across the typical range of building periods. They are thus used in initial building design. The structural force is defined as the

Table 1 Structural parameters and schematic model for single degree of freedom spectral analysis of **Analysis 2**. Stiffness is fixed, thus fixing device stiffness and forces, while mass is varied to achieve the desired structural period. There is 5% inherent structural damping



Structure Parameters:

- $K_S = 30,000 \text{ N/m}$
- **Mass** = varied to achieve desired period
- **Damping** = 5% inherent structural damping
- **Device** = as modeled

displacement times the column stiffness and is an indication of the required column strength and sizing. The total base shear is defined as the sum of the structural force and the resisting forces from the semi-active resettable device, and is an indication of the required foundation strength necessary for the device enhanced structure, which is critical given the high relative cost input of the foundations and difficulty in repairing or upgrading them once built.

More specifically, response spectra are generated from periods of 0.1 to 5.0s in 0.1s increments by changing the mass and using a model stiffness of 30,000 N/m and 5% structural damping. Note that the structural force spectrum is generated because the displacement response spectrum is equivalent to the structural force spectra scaled by column stiffness, and the resulting reduction factors are thus identical. The maximum response value is recorded for each period for each earthquake within the suit to generate the response spectra for every earthquake record for the baseline (no device, 5% internal viscous damping), and added device cases.

The results are then normalized to the uncontrolled baseline case, yielding a (multiplicative) reduction factor (RF) for each response metric. It is a measure of the change from baseline obtained by adding the device, and avoids issues with estimating modal parameter changes from noisy data (Huang *et al.* 2015). For a diamond shaped resettable device, the expected outcomes are further reduced displacement response compared to a 2-4 device case, but with increased base shear that still has a reduction factor of $RF < 1.0$. More specifically, a value of $RF > 1.0$ indicates a response greater than the structure with no device, and $RF < 1.0$ indicates a decrease in the response metric by the relevant RF multiplier.

4. Results and discussion

4.1 Analysis 1: Sinusoidal Inputs

Fig. 5 shows sinusoidal motion results for a 0.2 m amplitude input at periods of 5.0s, 1.0s and 0.1s (slow to

fast device velocity inputs). For each period, the force/displacement curve and the valve opening trajectories are plotted, noting that the valve delay is 0.01s.

In Fig. 5(a) with a 5.0s period, the diamond shape is nearly perfect with only a slight gap in quadrants 1 and 3 between the ideal reference force trajectory and the controlled case. Smooth valve opening and closing, seen in Fig. 5(a) (lower), shows no instability or saturation. In particular, the individual dots in Fig. 5(a) (lower) run together and are not clear due to the large period to valve delay ratio of 500 possible valve increments, where shorter periods in the other two plots have greater distinction. This case validates the fundamental ability of this active valve control to produce a diamond shape control law for the nonlinear device.

With a 1.0s period sinusoidal input, the quality of force tracking diminishes, as seen in Fig. 5(b). Sharp, rapid changes in force are required when transitioning at peak velocity when crossing zero and thus transitioning from quadrant 4 to quadrant 1 and from quadrant 2 to quadrant 3. This requirement combines with valve delay to cause the force to overshoot at these peaks. Hence, the active control valve cannot reduce the force as desired at these points to track the ideal reference input case. The results are worse, as might be expected, for the even faster sinusoidal input with 0.1s period.

More specifically, as the input motion period gets shorter with a valve delay of 0.01 seconds, the period/valve delay ratio becomes non-negligible with respect to the device dynamics and ability of the working fluid to respond to active chamber pressure. For an input period of 5.0s, a 0.01s valve delay offers the feedback controller 500 possible corrections for each cycle or 125 per quadrant. At 1.0s period, 100 (25 per quadrant) are available. Finally at 0.1s period only 10 corrections can be made. Each change reduces tracking ability, as evident in Fig. 5. Hence, for a 1.0s input motion period, with this valve delay of 0.01 sec, which is relatively quite small for this type of application, there is little ability to produce the desired ideal diamond shape. Thus, the controller is essentially unstable/ineffective with this 0.01s valve delay for periods below 1.0s.

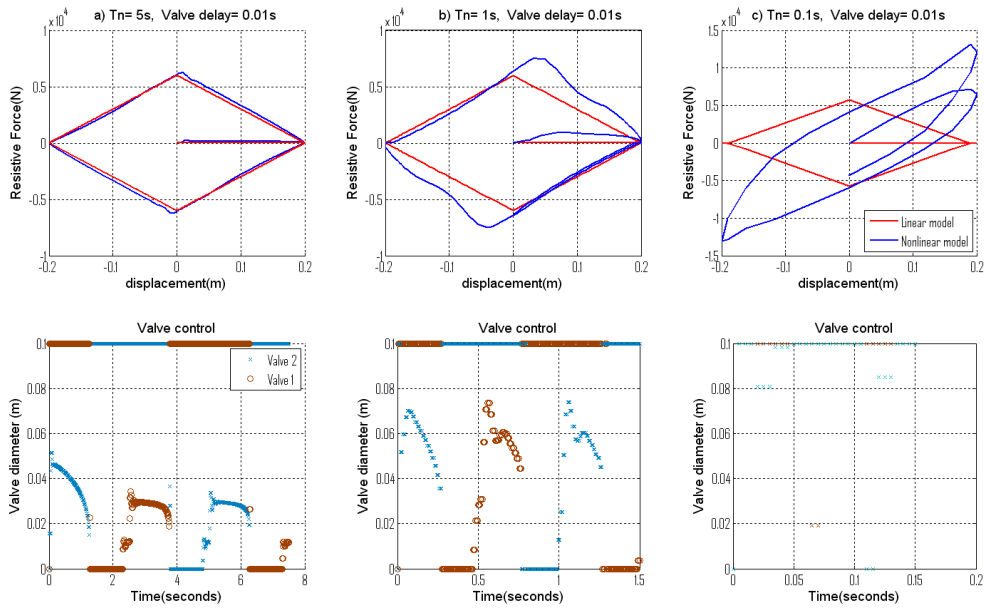


Fig. 5 Force/displacement and Valve opening for sinusoidal motion input of 0.2 m amplitude and period of 5.0, 1.0 and 0.1s (left to right). Valve delay of 0.01s

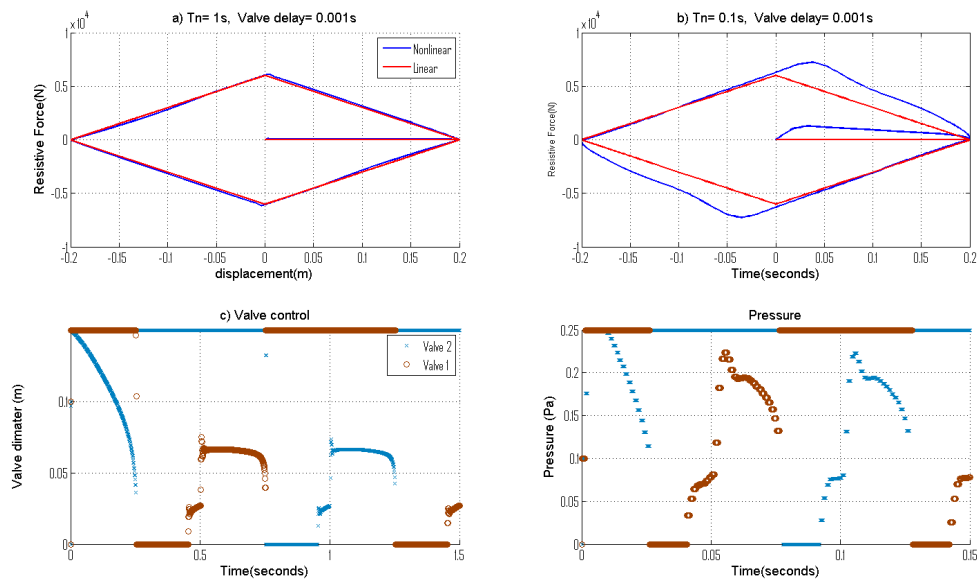


Fig. 6 Force/displacement and valve opening for sinusoidal motion input of 0.2 m amplitude and period of 1.0 and 0.1s. Valve delay of 0.001s. Tracking force is red and device force is blue

More importantly, it is clear that valve delay is the limiting factor in the tracking performance using this approach, rather than any controller inability resulting from using a simpler (PD) form of control.

Fig. 6 shows the same results for input motion periods of 0.1sec and 1.0sec but with a 10x smaller valve delay of 0.001s to validate this conclusion. As expected, for a 1.0s period (Fig. 6(a)) with 1000 possible corrections possible per cycle with this smaller delay, there is now a nearly perfect diamond shape. Further, a largely acceptable diamond shape very similar to Fig. 5(b) is now available for the 0.1s period, given the 100 possible time points, also just

as in Fig. 5(b), to correct and control the tracking of this shape. Finally, note also that in Figs. 5 and 6, where this ratio is high, the lower panel shows the many possible correction points as a dense set of circles. As the ratio declines these points become farther apart, further illustrating how the control difficulty rises, matched with decreasing tracking ability in the upper panel.

It is important to note that many more complex forms of control, such as neuro-fuzzy or other nonlinear or model reference adaptive control methods, could be used to ameliorate the issues with valve delay for the sinusoidal input cases in Figs. 5 and 6. However, these controllers

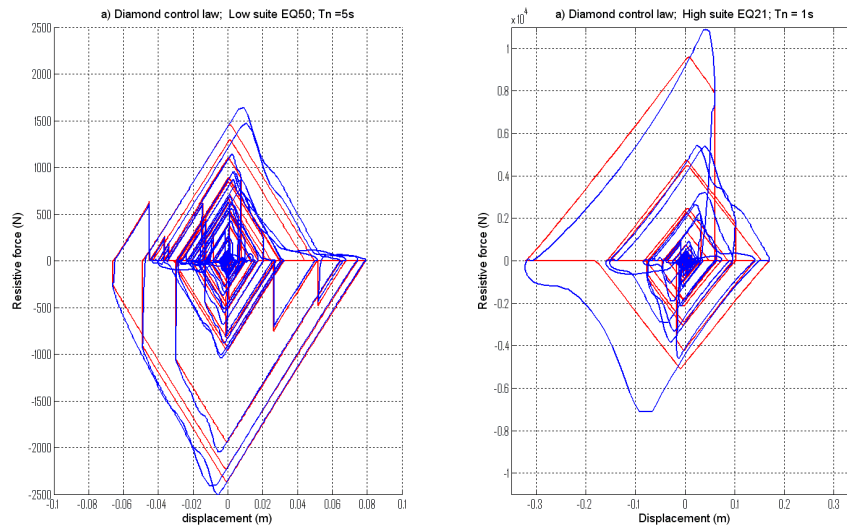


Fig. 7 Force/displacement plot for a single degree freedom structure of 5s natural period (5.a) under a low suite earthquake and 1s (5.b) under a high suite earthquake. Tracking force is red and device force is blue

would add significant complexity and potentially be less robust in regular use with such devices compared to the simpler approach used here. More importantly, such sinusoidal inputs are not what these devices typically experience, where earthquake ground motions are far more complex with several possible reversals mid-cycle, and, equally importantly, are unknown to the controller or control designer. Hence, valve delay is a major issue in these devices, as well as in semi-active MR devices (Katebi and Zadeh 2016).

4.2 Analysis 2: Random earthquake inputs and spectral analysis validation

Fig. 7 shows force-displacement results for 2 randomly selected earthquakes (of 60) of the SAC suites. The natural period is 5.0s for Fig. 7(a) (left) and 1.0s for Fig. 7(b) (right), spanning the typical range seen in most buildings for the first vibration mode that dominates response, and equally yielding slower and faster possible inputs to the device. The valve delay is 0.01s.

As expected, the ideal diamond shape is not as good in Fig. 7(b). However, both results are acceptable, as the active valve control shows no instability and never lost control of device force. Differences in quality between the 5.0s and 1.0s period structures in Figs. 7 are less significant than expected from the sinusoidal input results in Fig. 6. Nevertheless, at larger periods there is a better ability to track the desired force, as before, due to the greater number of time steps available to make, generally smaller, corrections to better track the desired reference input force.

For application focused validation, Figs. 8 and 9 show the RFs from spectral analysis for structural (equal to displacement scaled by stiffness) and base shear forces for both the realistic nonlinear device model and control, and an ideal, linear device model. This comparison measures ability to track and provide the ideal diamond shape control for random inputs across all periods. The results for both

cases are quite close over all periods, showing ability to effectively track the desired ideal linear case, across all the events with the nonlinear device model and control approach presented.

For the specific structural application case, the results show that given the ability to track the diamond shape reasonably well, the outcome RFs for base shear and structural force (equal to displacement response RF scaled by stiffness) are as expected for the proposed device hysteresis loop. Specifically, improved, lower RFs for structural force and thus displacement compared to the 2-4 case and closer to the 1-4 case, with similar to slightly higher base shear force RFs though still with values $RF < 1.0$.

Notably, base shear force RFs are also slightly larger (lesser reduction compared to the ideal case). This result is partly due to the overshoot of resistive forces into quadrants 1 and 3 with the given 0.01s valve delay, as seen in Fig. 5(b). This behavior is due to limited tracking ability seen in Fig. 5(b), and while a faster valve would rectify it as seen in Fig. 6, the overall outcome in this analysis with the slower valve has two main effects.

First, higher forces for a longer time, yield more dissipation area and a little more energy is dissipated, which contributes to further decreased displacement. Hence, at larger periods, where this effect is less important, reduction factors for the nonlinear, realistic modeled device are very close to the theoretically predicted ideal, linear model values. Second, for periods less than 1.0s significantly lower RF values are observed for the nonlinear case than expected from the ideal linear case because, before losing control, as in Fig. 5(c), at 0.2-0.3s periods, the overshoot is so dominant that the diamond shape control law looks more like a 1-4 control law than the ideal diamond shape, as expected from Figs. 5. Hence, the valve delay must be matched to the structural period for good, predictable results.

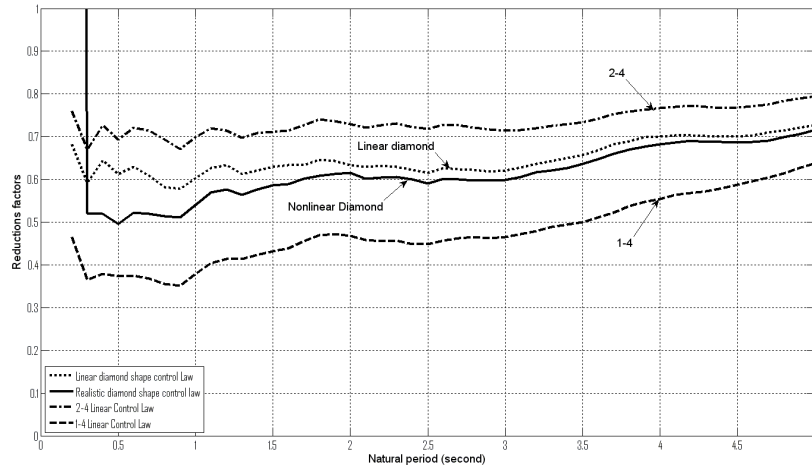


Fig. 8 Structural force RFs averaged across all 3 suites for each period for on/off control enabled 1-4 (Fig. 1(b)) and 2-4 (Fig. 1(c)) devices, as well as for the analog valve controlled “Diamond” device in both linear, ideal and nonlinear controlled cases. Displacement reductions factors are identical since structural force is displacement multiplied by the structural stiffness

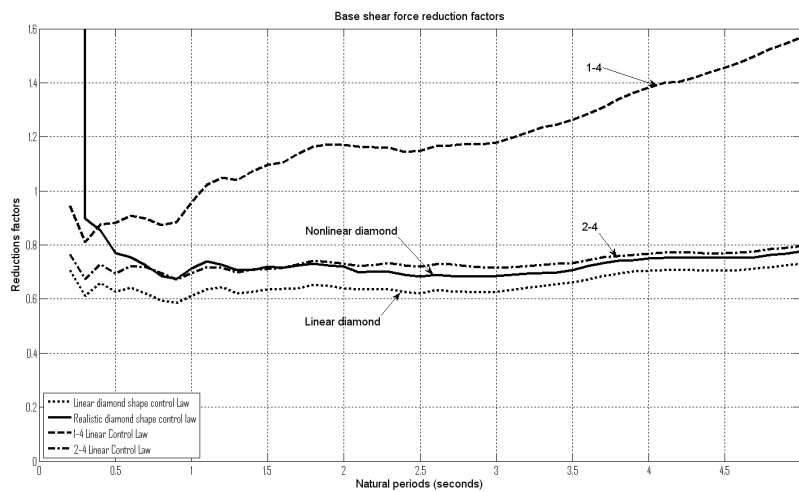


Fig. 9 Base shear force RFs averaged across all three suites for each period for on/off control enabled 1-4 (Fig. 1b) and 2-4 (Figure 1-c) devices, as well as for the analog valve controlled “Diamond” device in both linear, ideal and nonlinear controlled cases. Note that the 1-4 device has RF > 1.0 increasing base shear and foundation demand loads above a period of 1.0 sec

Finally, the diamond shaped control law is designed, conceptually, so that it does not increase base shear force. Overshoot of device resistive forces in quadrants 1 and 3 due to valve delay at small periods (high first mode frequency and thus faster response) of 0.2-0.3s, increases dissipation in these quadrants, but at the cost of potentially increasing base shear forces due to increased reaction loads at the foundation. Hence, higher base shear forces result from this interaction. However, faster valves, as discussed, could ameliorate this effect, and, in particular, using an array of very fast relatively low cost binary on/off valves would increase the valve speed and thus reduce the effective delay.

5. Conclusions

This work presents a design analysis illustrating the potential to control the energy release and resulting device force in nonlinear, fluid-based resettable semi-active devices using active valve control. It is based on an experimentally validated, highly non-linear device model and shows that a relatively simple PD control design can provide effective force tracking of ideal, linear device force-displacement loops, even under random and rapidly changing inputs like those seen in earthquake responses.

With respect to intended seismic application, this valve controlled device approach is currently the only way to enable a diamond shaped hysteresis loop in a semi-active

device, enabling several new application possibilities. The diamond-shaped device and control offer the advantages of a 2-4 device in terms of reduced, or non-increased, base shear reaction loads on the foundation, in concert with beneficial further reductions in displacement response. These results are demonstrated and validated across a range of structural periods and 60 ground motion inputs.

The results also clearly demonstrate that valve delay is the critical limiting factor. A sensitivity analysis of the impact of valve delay on the ability of the device controller to track the ideal linear inputs demanded, indicated that a minimum ratio of structural period to valve delay of 100-200 is required to achieve a consistent, almost ideal tracking for the structural and input motion periods of interest. This result generalises similarly to other more complex inputs, and is an equal and similar issue in MR and other devices. The result thus specifies the valve speed required at given device chamber pressures, enabling the validated model to also be used to determine the necessary device requirements, and a similar criterion is likely to be readily generalisable to MR and other devices.

Finally, the results and outcomes presented are readily generalised to similar semi-active devices. Equally, the control and device concepts presented illustrate the means by which the design space and potential of these resettable devices can be increased.

Acknowledgments

The research described in this paper was financially supported by the NZ Earthquake Commission Research Fund and the Royal Society of New Zealand Rutherford Fellowship fund.

References

- Barroso, L.R., Chase, J.G. and Hunt, S. (2003), "Resettable smart dampers for multi-level seismic hazard mitigation of steel moment frames", *J. Struct. Control*, **10**(1), 41-58.
- Beziat, A., Munoz, A.M., Chase, J.G., MacRae, G.A., Rodgers, G. W. and Clifton, C. (2012), "Performance analysis of energy dissipators and isolators placed in bridges to prevent structural damage in columns", *J. Earthq. Eng.*, **16**(8), 1113-1131.
- Bitaraf, M., Barroso, L.R. and Hurlebaus, S. (2010a), "Adaptive control to mitigate damage impact on structural response", *J. Intel. Mat. Syst. Str.*, **21**(6), 607-619.
- Bitaraf, M. and Hurlebaus, S. (2013), "Semi-active adaptive control of seismically excited 20-story nonlinear building", *Eng. Struct.*, **56**, 2107-2118.
- Bitaraf, M., Hurlebaus, S. and Barroso, L.R. (2012), "Active and semi-active adaptive control for undamaged and damaged building structures under seismic load", *Comput. - Aided Civil Infrastruct. Eng.*, **27**(1), 48-64.
- Bitaraf, M., Ozbulut, O.E., Hurlebaus, S. and Barroso, L. (2010b), "Application of semi-active control strategies for seismic protection of buildings with MR dampers", *Eng. Struct.*, **32**(10), 3040-3047.
- Bobrow, J.E., Jabbari, F. and Thai, K. (2000), "A new approach to shock isolation and vibration suppression using a resettable actuator", *ASME Transactions on Dynamic Systems, Measurement, and Control.*, **122**(3), 570-573.
- Caterino, N., Spizzuoco, M. and Occhiuzzi, A. (2015), "Shaking table testing of a steel frame structure equipped with semi-active MR dampers: comparison of control algorithms", *Smart Struct. Syst.*, **15**(4), 963-995.
- Chase, J.G., Barroso, L.R. and Hunt, S. (2004), "The impact of total acceleration control for semi-active earthquake hazard mitigation", *Eng. Struct.*, **26**(2), 201-209.
- Chase, J.G., Mulligan, K.J., Gue, A., Alnot, T., Rodgers, G., Mander, J.B., Elliott, R., Deam, B., Cleeve, L. and Heaton, D. (2006), "Re-shaping hysteretic behaviour using semi-active resettable device dampers", *Eng. Struct.*, **28**(10), 1418-1429.
- Chen, X.Q., Chase, J.G., Mulligan, K.J., Rodgers, G.W. and Mander, J.B. (2008), "Novel controllable semiactive-devices for reshaping structural response", *Ieee-Asme Transactions on Mechatronics*, **13**, 647-657.
- Chen, Z.H., Ni, Y.Q. and Or, S.W. (2015), "Characterization and modeling of a self-sensing MR damper under harmonic loading", *Smart Struct. Syst.*, **15**(4), 1103-1120.
- Chopra, A.K. (1995), *Dynamics of structures : Theory and applications to earthquake engineering*.
- Dyke, S.J. and Spencer, B.F. (1996), "Modeling and control of magnetorheological dampers for seismic response reduction", *Smart Mater. Struct.*, **5**(5), 565-575.
- Esteki, K., Bagchi, A. and Sedaghti, R. (2015), "Semi-active control of seismic response of a building using MR fluid-based tuned mass damper", *Smart Struct. Syst.*, **16**(5), 807-833.
- Ewing, C.M., Guillin, C., Dhakal, R.P. and Chase, J.G. (2009), "Spectral analysis of semi-actively controlled structures subjected to blast loading", *Struct. Eng. Mech.*, **33**(1), 79-93.
- Feng, M.Q. (1993), "Application of hybrid sliding isolation system to buildings", *J. Eng. Mech. - ASCE*, **119**(10), 2090-2108.
- Feng, M.Q., Shinozuka, M. and Fujii, S. (1993), "Friction-controllable sliding isolation system", *J. Eng. Mech. - ASCE*, **119**, 1845-1864.
- Huang, Q.D., Gardoni, P. and Hurlebaus, S. (2015), "Assessment of modal parameters considering measurement and modeling errors", *Smart Struct. Syst.*, **15**, 717-733.
- Jabbari, F. and Bobrow, J.E. (2002), "Vibration suppression with a resettable device", *J. Eng. Mech. - ASCE*, **128**(9), 916-924.
- Jansen, L.M. and Dyke, S.J. (2000), "Semiactive control strategies for MR dampers: Comparative study", *J. Eng. Mech. - ASCE*, **126**(8), 795-803.
- Katebi, J. and Zadeh, S.M. (2016), "Time delay study for semi-active control of coupled adjacent structures using MR damper", *Struct. Eng. Mech.*, **58**(6), 1127-1143.
- Kim, Y., Langari, R. and Hurlebaus, S. (2010), "Control of a seismically excited benchmark building using linear matrix inequality-based semiactive nonlinear fuzzy control", *J. Struct. Eng. - ASCE*, **136**(8), 1023-1026.
- Kori, J.G. and Jangid, R.S. (2008), "Semi-active friction dampers for seismic control of structures", *Smart Struct. Syst.*, **4**(4), 493-515.
- Maiti, D.K., Shyju, P.P. and Vijayaraju, K. (2006), "Vibration control of mechanical systems using semi-active MR-damper", *Smart Struct. Syst.*, **2**(1), 61-80.
- Makris, N. and Chang, S.P. (2000), "Effect of viscous, viscoplastic and friction damping on the response of seismic isolated structures", *Earthq. Eng. Struct. D.*, **29**, 85-107.
- Mulligan, K.J. (2007), *Experimental and analytical studies of semi-active and passive structural control of buildings*, PhD, University of Canterbury.
- Mulligan, K.J., Chase, J.G., Mander, J.B., Rodgers, G.W. and Elliott, R.B. (2010), "Nonlinear models and validation for resettable device design and enhanced force capacity", *Struct. Control Health Monit.*, **17**(3), 301-316.
- Mulligan, K.J., Chase, J.G., Mander, J.B., Rodgers, G.W., Elliott, R.B., Franco-Anaya, R. and Carr, A.J. (2009), "Experimental

- validation of semi-active resettable actuators in a 1/5th scale test structure”, *Earthq. Eng. Struct. D.*, **38**, 517-536.
- Nagarajaiah, S. and Jung, H. J. (2014), “Smart tuned mass dampers: recent developments”, *Smart Struct. Syst.*, **13**, 173-176.
- Ozbulut, O.E., Bitaraf, M. and Hurlebaus, S. (2011), “Adaptive control of base-isolated structures against near-field earthquakes using variable friction dampers”, *Eng. Struct.*, **33**(12), 3143-3154.
- Ozbulut, O.E. and Hurlebaus, S. (2010), “Fuzzy control of piezoelectric friction dampers for seismic protection of smart base isolated buildings”, *Bull. Earthq. Eng.*, **8**(6), 1435-1455.
- Ozbulut, O.E. and Hurlebaus, S. (2011a), “Energy-balance assessment of shape memory alloy-based seismic isolation devices”, *Smart Struct. Syst.*, **8**(4), 399-412.
- Ozbulut, O.E. and Hurlebaus, S. (2011b), “Re-centering variable friction device for vibration control of structures subjected to near-field earthquakes”, *Mech. Syst. Signal Pr.*, **25**(8), 2849-2862.
- Ozbulut, O.E. and Hurlebaus, S. (2012a), “Application of an SMA-based hybrid control device to 20-story nonlinear benchmark building”, *Earthq. Eng. Struct. D.*, **41**(13), 1831-1843.
- Ozbulut, O.E. and Hurlebaus, S. (2012b), “A comparative study on the seismic performance of superelastic-friction base isolators against Near-Field Earthquakes”, *Earthq. Spectra*, **28**(3), 1147-1163.
- Ramallo, J.C., Johnson, E.A. and Spencer, B.F. (2002) “ ‘Smart’ base isolation systems”, *J. Eng. Mech. - ASCE*, **128**(10), 1088-1099.
- Rodgers, G.W., Mander, J.B., Chase, J.G., Mulligan, K.J., Deam, B.L. and Carr, A. (2007), “Re-shaping hysteretic behaviour - spectral analysis and design equations for semi-active structures”, *Earthq. Eng. Struct. D.*, **36**(1), 77-100.
- Som, A., Kim, D.H. and Son, H.S. (2015), “Semiactive magnetorheological damper for high aspect ratio boring process”, *Ieee-Asme Transactions on Mechatronics*, **20**(5), 2575-2582.
- Sommerville, P., Smith, N., Punyamurthula, S. and Sun, J. (1997), “Development of Ground Motion Time Histories For Phase II Of The FEMA/SAC Steel Project, SAC Background Document Report SAC/BD-97/04.
- Spencer, B.F., Dyke, S.J., Sain, M.K. and Carlson, J. (1997), “Phenomenological model of magnetorheological damper”, *J. Eng. Mech. - ASCE*, **123**(3), 230-238.
- Spencer, B.F., Johnson, E.A. and Ramallo, J.C. (2000), “ ‘Smart’ isolation for seismic control”, *Int. J. Series C-Mech. Syst. Machine Elem. Manufact. - Jsme*, **43**, 704-711.
- Sun, C., Nagarajaiah, S. and Dick, A.J. (2014), “Family of smart tuned mass dampers with variable frequency under harmonic excitations and ground motions: closed-form evaluation”, *Smart Struct. Syst.*, **13**(2), 319-341.
- Woo, S.S., Lee, S.H. and Chung, L. (2011), “Seismic response control of elastic and inelastic structures by using passive and semi-active tuned mass dampers”, *Smart Struct. Syst.*, **8**(3), 239-252.
- Yang, J.N. and Agrawal, A.K. (2002), “Semi-active hybrid control systems for nonlinear buildings against near-field earthquakes”, *Eng. Struct.*, **24**(3), 271-280.
- Yang, J.N., Bobrow, J., Jabbari, F., Leavitt, J., Cheng, C.P. and Lin, P.Y. (2007), “Full-scale experimental verification of resettable semi-active stiffness dampers”, *Earthq. Eng. Struct. D.*, **36**(9), 1255-1273.
- Zhang, J.Q. and Agrawal, A.K. (2015), “An innovative hardware emulated simple passive semi-active controller for vibration control of MR dampers”, *Smart Struct. Syst.*, **15**(3), 831-846.
- Zhou, Z., Meng, S.P., Wu, J. and Zhao, Y. (2012), “Semi-active control on long-span reticulated steel structures using MR dampers under multi-dimensional earthquake excitations”, *Smart Struct. Syst.*, **10**(6), 557-572.

HJ